

GYROSCOPE ARCHITECTURE WITH STRUCTURALLY FORCED ANTI-PHASE DRIVE-MODE AND LINEARLY COUPLED ANTI-PHASE SENSE-MODE

A.A. Trusov, A.R. Schofield, and A.M. Shkel*

MicroSystems Laboratory, University of California, Irvine, CA, USA

ABSTRACT

This paper reports, for the first time, a vibratory MEMS z-axis rate gyroscope architecture with structurally forced anti-phase drive-mode and linearly coupled, dynamically balanced anti-phase sense-mode. The new design utilizes two symmetrically-decoupled tines with drive- and sense-mode synchronization mechanisms, and prioritizes sense-mode quality factor. The levered drive-mode mechanism structurally forces the anti-phase drive-mode motion and eliminates the lower frequency spurious modes. The linearly coupled, dynamically balanced anti-phase sense-mode design minimizes substrate energy dissipation. SOI prototypes characterized in vacuum demonstrated drive-mode quality factor of 67,000 and ultra-high sense-mode quality factor of 125,000, yielding mechanical scale factor of 0.4 nm/(°/h) for mode-matched operation.

KEYWORDS

Vibratory gyroscope, tuning fork, high-Q design

INTRODUCTION

The operation of micromachined vibratory gyroscopes is based on a transfer of energy between two modes of vibration caused by the Coriolis effect [1]. When the drive-mode and sense-mode resonant frequencies are equal, or mode-matched, the sensor output is increased proportionally to the sense-mode quality factor [2]. Anti-phase driven tuning fork architectures are often used due to their ability to reject common mode acceleration inputs [3]. Conventional tuning fork designs with linear anti-phase drive-modes present two major drawbacks: presence of the parasitic low-frequency structural mode of in-phase vibrations [4] and limitation of the maximal achievable sense-mode quality factor by approximately half of the drive-mode quality factor [5] due to substrate energy dissipation caused by the torque imbalance [6].

In this paper, we introduce a new tuning fork architecture addressing the limitations of the conventional designs. The spurious in-phase drive-mode is shifted above the operational frequency to improve response characteristics. Unlike conventional tuning fork gyroscopes, the proposed architecture prioritizes the quality factor of the sense-mode by mechanical design, where the linearly coupled anti-phase sense-mode is balanced in both the linear momentum as well as moment of reaction forces (torque) in order to minimize dissipation of energy through the substrate and enable ultra-high mechanical sensitivity to the input angular rate.

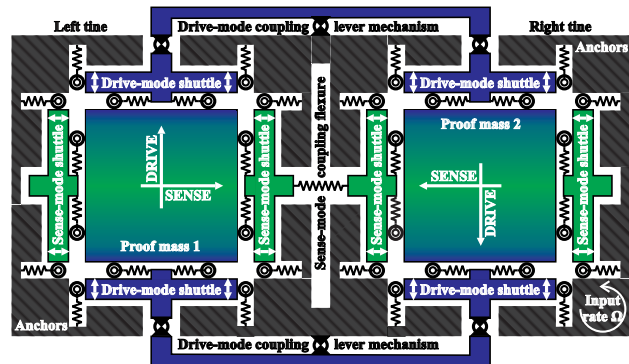


Figure 1: Structural schematic of the proposed gyroscope architecture with levered anti-phase drive-mode and linearly coupled anti-phase sense-mode for maximization of sense-mode Q -factor.

DESIGN CONCEPT

The proposed mechanical architecture, Fig. 1, comprises two identical tines, a lever mechanism for synchronization of the anti-phase drive-mode motion, and coupling flexures for the linear anti-phase sense-mode. Each tine consists of an anchored outer frame, two drive-mode and two sense-mode shuttles [7], and a proof mass. The drive-mode and sense-mode shuttles are suspended in the x - y plane relative to the substrate by pairs of springs. These flexures restrict the motion of the shuttles solely to their respective axes. Suspension elements of identical geometry couple the shuttles to their respective proof masses. Proof masses of both tines are suspended in the x - y plane with equal effective stiffnesses. The symmetry of the tines improves robustness of drive- and sense-mode frequency positioning (the two resonant frequencies are maintained equal in the mode-matched case) to fabrication imperfections and temperature induced shifts of resonant frequencies.

Drive-Mode Design

The drive-mode of the gyroscope is formed by the two tines forced into anti-parallel, anti-phase motion synchronized by the mechanical system that allows angular displacement of the coupling levers with respect to the anchored pivot, Fig. 2. Rigidity of the levering mechanism to the in-phase displacement eliminates any lower-frequency modes of vibration and shifts the in-phase drive-mode above the operational frequency of the device, Fig. 3. The intentional mode arrangement improves the phase stability [4] and guarantees common mode rejection.

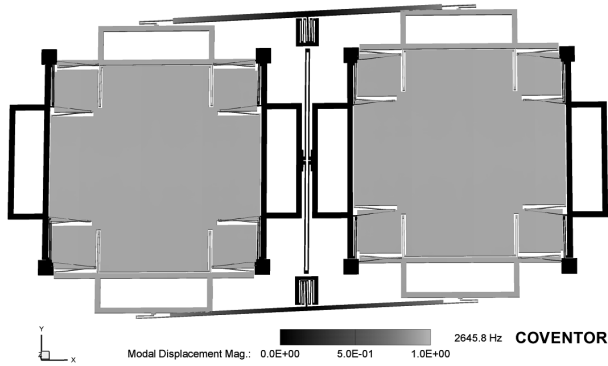


Figure 2: Levered anti-phase drive-mode (FEM).

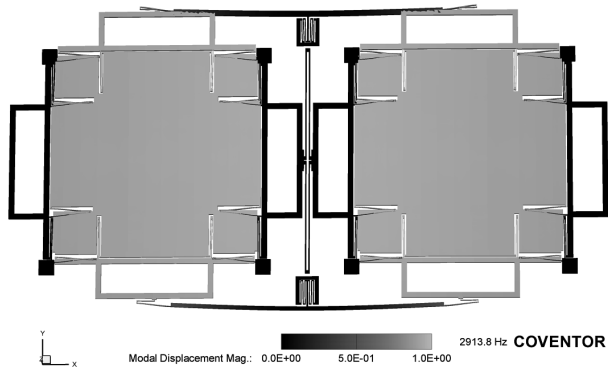


Figure 3: In-phase drive-mode resonance is shifted to a higher frequency by the mechanical structure design (FEM).

Sense-Mode Design

The sense-mode of the gyroscope is formed by the two linearly coupled tines moving in anti-phase to each other in response to the anti-phase Coriolis input, Fig. 4. While achieving high sense-mode quality factors is essential to improve sensitivity and precision of vibratory gyroscopes, the quality factors of vibrating microstructures in vacuum are often limited by the dissipation of energy through the substrate due to linear momentum and torque imbalances [6]. Unlike conventional tuning fork gyroscopes, the proposed architecture prioritizes the quality factor of the sense-mode by mechanical design, where the linearly coupled anti-phase sense-mode is balanced in both the linear momentum as well as torque in order to minimize the dissipation of energy through the substrate.

Actuation and Detection

The gyroscope is electrostatically driven into anti-phase motion using driving voltages imposed across the differential lateral comb electrodes on the drive-mode shuttles. During rotation around the z -axis, the Coriolis acceleration of the proof masses induces linear anti-phase sense-mode vibrations which are capacitively detected using differential parallel plate electrodes on the sense-mode shuttles.

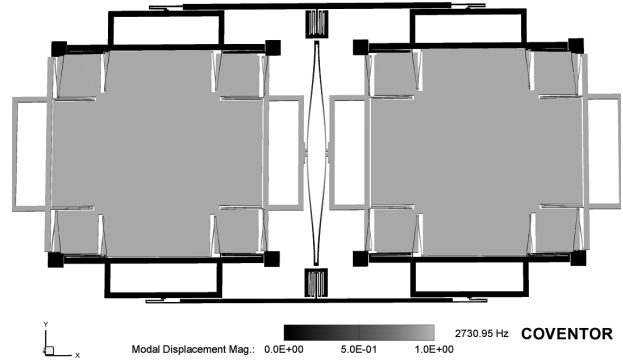


Figure 4: Linearly coupled anti-phase sense-mode (FEM). Momentum and torque balance minimizes dissipation of energy through the substrate for ultra high sense-mode quality factor.

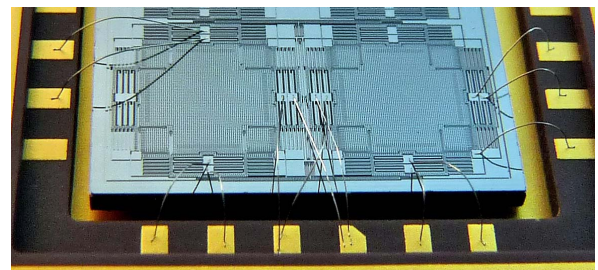


Figure 5: Optical photograph of a packaged tuning fork gyroscope. Differential wirebonds are visible.

EXPERIMENTAL CHARACTERIZATION

In this section we report experimental characterization of micromachined prototypes of the proposed architecture.

Prototype Fabrication

The fabrication of prototypes was done using an in-house, wafer-level, single-mask process using silicon-on-insulator (SOI) wafers with a $50\ \mu\text{m}$ thick device layer and a $5\ \mu\text{m}$ buried oxide layer. After patterning photoresist with the device mask, the wafers were subjected to a Deep Reactive Ion Etching (DRIE) using a Surface Technology Systems (STS) Advanced Silicon Etching (ASE) tool. The minimal feature of $5\ \mu\text{m}$ was used to define capacitive gaps. The perforated structures were released using a timed 20% HF acid bath. For convenient characterization individual devices were packaged using ceramic DIP-24 packages and wirebonded as illustrated in Fig. 5.

Structural Characterization

Structural characterization of a prototype operated in air is shown in Fig. 6. As predicted by the modeling, the anti-phase levered operational mode at 2,483 Hz is the lowest frequency mode along the drive direction, while all the spurious modes are shifted to higher frequencies. For the tested prototype, the in-phase drive-mode is at 2,781 Hz, which can be increased even farther by stiffening the u-shaped flexures located at the tips of the drive-mode

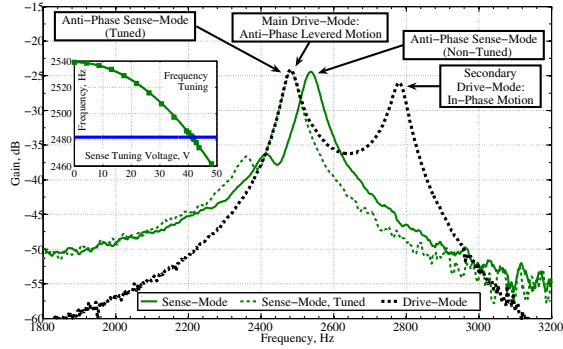


Figure 6: Measured frequency responses of the drive- and the sense-modes in air. Inset: frequency tuning for mode-matching.

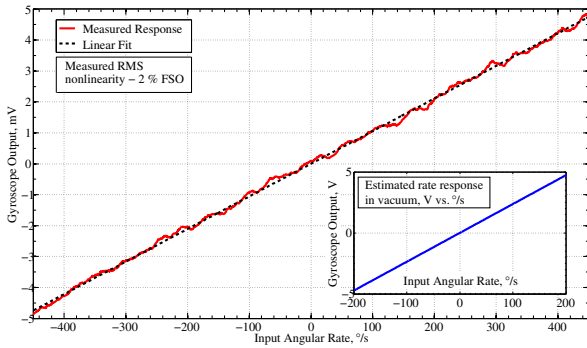


Figure 7: Measured rate response at atmospheric pressure (sense-mode quality factor 65, RMS nonlinearity 2 % FSO). Sensitivity improves more than 2,000 times in vacuum.

synchronization levers. The untrimmed anti-phase sense-mode resonance was measured at 2,538 Hz, which is 55 Hz above the drive-mode operational frequency. The device can be operated in air without frequency tuning providing a practically feasible bandwidth on the order of 50 Hz. For high-sensitivity, mode-matched operation at reduced pressures, the sense-mode resonance is tuned down to 2,483 Hz using the negative electrostatic spring effect as shown in the inset of Fig. 6.

Rate Characterization

The angular rate performance of the prototype was experimentally characterized in air using a computer-controlled Ideal Aeromsmith 1291BR rate table. The gyroscope was driven into the anti-phase resonant motion with a 5 μm amplitude using a combination of a 30 V DC bias and a 3.5 Vrms AC driving voltage applied to the anchored differential drive-mode lateral-comb electrodes. Differential electro-mechanical amplitude modulation (EAM) technique [8] was used to detect the Coriolis-induced motion in the sense-mode. The AC carrier voltage with 3.5 Vrms amplitude at 80 kHz frequency was applied to the mobile masses. The anchored differential sense-mode parallel-plate electrodes were connected to the inputs of a two-stage differential transimpedance amplification circuit.

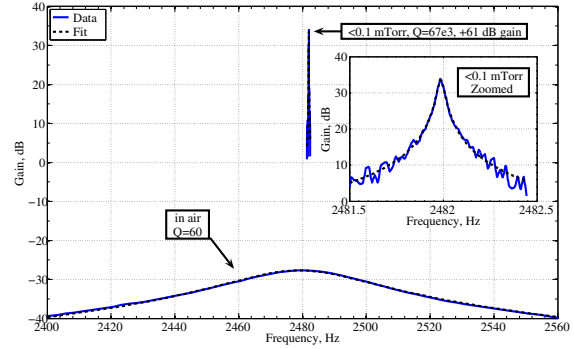


Figure 8: Measured frequency response of the levered anti-phase drive-mode in air ($Q=60$), and in vacuum ($Q=67,000$).

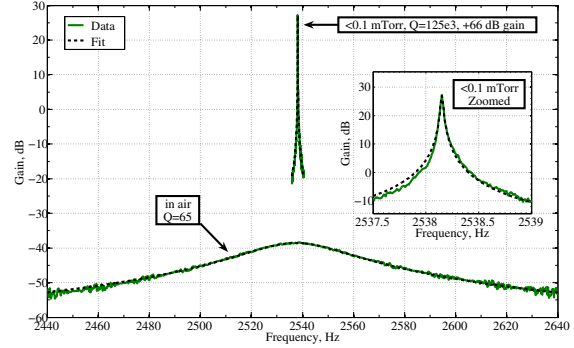


Figure 9: Measured frequency response of the momentum and torque balanced linear anti-phase sense-mode in air ($Q=65$), and in vacuum ($Q=125,000$).

An experimentally measured rate response of the prototype in atmospheric pressure is shown in Fig. 7, confirming Coriolis functionality of the proposed mechanical sensor element architecture.

Ultra-High Quality Factor Operation

The limiting non-viscous quality factors of the drive- and sense-modes were characterized using a custom vacuum chamber pumped to approximately 0.1 mTorr in order to eliminate effects of gas damping. As shown in Fig. 8, the measured quality factor of the drive-mode in vacuum increases to 67,000, which allows driving the gyroscope with just 3 mVrms AC driving voltage combined with a 30 V DC polarization voltage. While the anti-parallel, anti-phase drive-mode is balanced in linear momentum, the quality factor is limited by the dissipation of energy through the substrate due to the non-zero torque. In contrast, as shown in Fig. 9, the measured limiting quality factor of the sense-mode reaches 125,000 due to the energy dissipation optimized mechanical design.

A single-mass gyroscope identical to one uncoupled tine was also fabricated and characterized to analyze the advantages of the proposed tuning fork architecture. For a single mass device, the limiting non-viscous quality factor of both the drive- and the sense-mode is 10,000, as shown

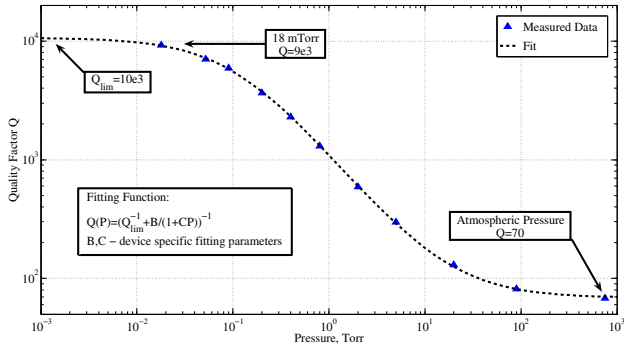


Figure 10: Measured quality factor versus pressure for an individual, uncoupled tine. The quality factor in vacuum is limited to 10,000 by the energy dissipation through the substrate caused by the momentum imbalance.

in Fig 10. Momentum balance of the tuning fork drive-mode results in a 6.7 times improvement of the quality factor; momentum and torque balance of the tuning fork sense-mode allows a 12.5 times improvement in quality factor and sensitivity.

The ultra high quality factor of the sense-mode translates into more than two thousand times sensitivity improvement for the gyroscope operated in vacuum, Fig. 11. Even further increase of the sense-mode quality factor is achieved by tightening the fabrication tolerances and employing more rigid die attachment, such as eutectic bonding using solder preforms [6].

CONCLUSIONS

We demonstrated a new tuning fork gyroscope design architecture, which utilizes symmetrically decoupled tines with drive- and sense- mode synchronization structures. The levered drive-mode mechanism structurally forces the anti-parallel, anti-phase drive-mode motion and eliminates the lower frequency spurious modes present in conventional tuning fork gyroscopes. The linearly coupled, momentum and torque balanced anti-phase sense-mode reduces dissipation of energy through the substrate yielding ultra high quality factors. Prototypes characterized in vacuum demonstrated drive-mode quality factor of 67,000 and ultra-high sense-mode quality factor of 125,000 resulting in mechanical rate sensitivity of 0.4 nm/(°/h) of input rate. The new tuning fork architecture has potential in applications such as gyrocompassing, where ultra-high precision inertial measurements are required in a relatively low bandwidth.

ACKNOWLEDGMENTS

This work was supported by the National Science Foundation grant CMS-0409923 and Naval Surface Warfare Center contract N00178-08-C1014. The authors would like to acknowledge University of California, Irvine Integrated Nanosystems Research Facility (INRF) for as-

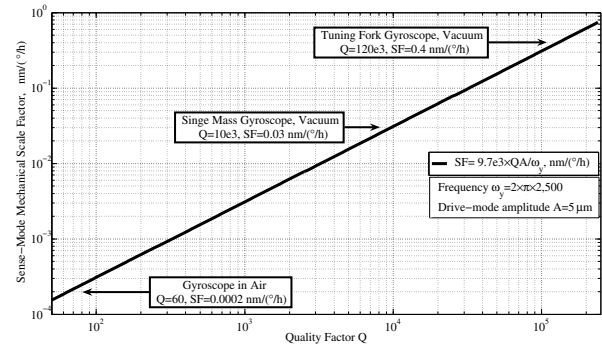


Figure 11: Simulated scale factor of the gyroscope as a function of the sense-mode quality factor.

stance with the fabrication of prototypes. The gyroscopes were designed and characterized at the Microsystems Laboratory, University of California, Irvine.

REFERENCES

- [1] A.M. Shkel, "Type I and Type II Micromachined Vibratory Gyroscopes," in *Proc. of IEEE/ION PLANS*, San Diego, CA, USA, April 24-27, 2006.
- [2] N. Yazdi, F. Ayazi and K. Najafi, "Micromachined Inertial Sensors," *Proc. IEEE*, vol. 86, no. 8, pp. 1640–1659, August 1998.
- [3] M. Weinberg and A. Kourepenis, "Error Sources in In-Plane Silicon Tuning-Fork MEMS Gyroscopes," *J. Microelectromech. Syst.*, vol. 15, no. 3, pp. 479–491, June 2006.
- [4] K. Azgin, Y. Temiz, T. Akin, "An SOI-MEMS Tuning Fork Gyroscope with Linearly Coupled Drive Mechanism," in *Proc. IEEE MEMS 2007 Conference*, Kobe, Japan, pp.607-610, January 21-25, 2007.
- [5] M.F. Zaman, A. Sharma, Z. Hao, F. Ayazi, "A Mode-Matched Silicon-Yaw Tuning-Fork Gyroscope with Subdegree-per-Hour Allan Deviation Bias Instability," *J. Microelectromech. Syst.*, vol.17, no.6, pp.1526-1536, December 2008.
- [6] A.A. Trusov, A.R. Schofield, A.M. Shkel, "A Substrate Energy Dissipation Mechanism in In-Phase and Anti-Phase Micromachined Z-Axis Vibratory Gyroscopes", *JMM*, vol. 18, pp. 095016(10), September 2008.
- [7] M.S. Kranz, G.K. Fedder, "Micromechanical Vibratory Rate Gyroscopes Fabricated in Conventional CMOS," in *Proc. Symposium Gyro Technology 1997*, Stuttgart, Germany, pp. 3.0–3.8., September 16-17, 1997.
- [8] A.A. Trusov, A.M. Shkel, "Capacitive Detection in Resonant MEMS with Arbitrary Amplitude of Motion," *JMM*, vol. 17 (8), pp. 1583–1592, July 2007.

CONTACT

* A.A. Trusov, tel: +1-949-824-6314; atrusov@uci.edu.